4486 *Inorg. Chem.* **2010**, *49*, 4486–4490
DOI: 10.1021/ic902211c

Inorganic Chemistry
Article

Molten Salt Synthesis and Structural Characterization of Novel Salt-Inclusion Vanadium Bronze $Cs_5FeV_5O_{13}Cl_6$

Parisa Mahjoor and Susan E. Latturner*

Department of Chemistry and Biochemistry, Florida State University, Tallahassee, Florida 32306

Received November 9, 2009

Single crystals of a new reduced vanadate phase, $Cs_5FeV_5O_{13}Cl_6$, have been grown from the reaction of metal oxides V_2O_5 and Fe_2O_3 in the presence of a metal reducing agent in a eutectic CsCl/NaCl flux. This compound adopts a tetragonal structure (*P*4/*nmm*, *a* = 10.943(3) Å, *c* = 10.535(4) Å, Z = 2) that consists of reduced vanadate layers separated by ionic layers comprised of $[FeCl_6]^{3-}$ anions and Cs^+ cations. There are two distinct vanadium sites in the structure of this compound; V^{4+} is in square pyramidal configuration, and V^{5+} has a tetrahedral coordination environment. The ^{51}V NMR Knight shift and the magnetic susceptibility data indicate the delocalization of the unpaired electron of vanadium. Ferrimagnetic ordering is observed at 5 K.

Introduction

Molten salts are a powerful tool in materials synthesis because their wide electrochemical window allows for the production of unusual valence states and ionic species which would be unstable in traditional solvents. The solubility of metal oxides in molten salts has facilitated the synthesis of a variety of new complex oxide compounds, such as transition-metal phosphates, arsenates, and silicates.[1−5] These compounds exhibit covalently bonded metal oxide frameworks, some of which are templated by occlusion of salt clusters ("salt inclusion solids").[6−10] The low melting point and acid−base chemistry of hydroxide salts have made them attractive media for the synthesis of layered cuprates and tantalates;[11−13] the presence of the O^{2-} anion in the melt stabilizes metal ions in high oxidation states. On the other hand, the use of halide salt fluxes can facilitate crystallization of reduced phases; for instance, the reaction of Ti and $CaTiO_3$ in $CaCl_2$ produces a reduced titanate, $CaTi_2O_4$.[14,15] In this vein, we are exploring the reduction of vanadium and molybdenum oxides in metal halide flux mixtures to crystallize new transition-metal bronze phases.

Transition-metal bronzes, $A_xM_yO_z$ (M = Ti, Nb, Mo, W, Re, V, and Ta and A = H, NH_4^+, alkali, alkaline earth, or rare earth metal), are oxide compounds containing early transition metals in lower than normal oxidation states. The A cations are incorporated into the vacancies of the M_yO_z oxide structure. By varying the size and concentration of A cations, a large number of $A_xM_yO_z$ phases with different compositions can be obtained. The A cation donates its valence electron to the usually empty transition-metal d-orbital derived conduction band. Transport and optical properties of bronzes, therefore, depend on the extent of d-orbital overlap, which determines the bandwidth and the delocalization of the d-electrons.[16] It has been confirmed by several experiments that the orbitals of the A cation do not contribute to the formation of these levels. Vanadium bronzes are of particular interest; vanadium ions can exhibit octahedral, tetrahedral, trigonal, or square pyramidal oxygen coordination, and these polyhedra show a strong tendency to

*Corresponding author. E-mail: latturne@chem.fsu.edu.

(1) Etheredge, K. M. S.; Hwu, S.-J. *Inorg. Chem.* **1995**, *34*, 3123–3125.
(2) Huang, Q.; Ulutagay, M.; Michener, P. A.; Hwu, S.-J. *J. Am. Chem. Soc.* **1999**, *121*, 10323–10326.
(3) Huang, Q.; Hwu, S.-J. *Inorg. Chem.* **2003**, *42*, 655–657.
(4) Mueller, A.; Reuter, H.; Dillinger, S. *Angew. Chem., Int. Ed.* **1995**, *34*, 2328–61.
(5) Ulutagay, M.; Schimek, G. L.; Hwu, S.-J.; Taye, H. *Inorg. Chem.* **1998**, *37*, 1507–1512.
(6) Queen, W. L.; West, J. P.; Hwu, S.-J.; VanDerveer, D. G.; Zarzyczny, M. C.; Pavlick, R. A. *Angew. Chem., Int. Ed.* **2008**, *47*, 3791–3794.
(7) Rettich, R.; Muller-Buschbaum, H. *Z. Naturforsch., B: J. Chem. Sci.* **1997**, *52*, 457–461.
(8) Liao, C.-H.; Chang, P.-C.; Kao, H.-M.; Lii, K.-H. *Inorg. Chem.* **2005**, *44*, 9335–9339.
(9) Hwu, S.-J.; Ulutagay-Kartin, M.; Clayhold, J. A.; Mackay, R.; Wardojo, T. A.; O'Connor, C. J.; Krawiec, M. *J. Am. Chem. Soc.* **2002**, *124*, 12404–5.
(10) Huang, Q.; Kartin, M.; Mo, X.; Hwu, S.-J., *Mater. Res. Soc. Symp. Proc.* **2002**, *755*, (Solid-State Chemistry of Inorganic Materials IV), 459-464.
(11) (a) Sunshine, S. A.; Siegrist, T.; Schneemeyer, L. F. *J. Mater. Res.* **1997**, *12*, 1210–1213. (b) Stoll, S. L.; Stacy, A. M.; Torardi, C. C. *Inorg. Chem.* **1994**, *33*, 2761–2765.
(12) Schmachtel, J.; Mueller-Buschbaum, H. *Z. Anorg. Allg. Chem.* **1981**, *472*, 89–94.
(13) (a) Roof, I. P.; Smith, M. D.; Cussen, E. J.; zur Loye, H. C. *J. Solid State Chem.* **2009**, *182*, 295–300. (b) Mugavero, S. J.; Gemmill, W. R.; Roof, I. P.; Zur Loye, H. C. *J. Solid State Chem.* **2009**, *182*, 1950–1963.
(14) Geselbracht, M. J.; Noailles, L. D.; Ngo, L. T.; Pikul, J. H.; Walton, R. I.; Cowell, E. S.; Millange, F.; O'Hare, D. *Chem. Mater.* **2004**, *16*, 1153–1159.
(15) Rogge, M. P.; Cladwell, J. H.; Ingram, D. R.; Green, C. E.; Geselbracht, M. J.; Siegrist, T. *J. Solid State Chem.* **1998**, *141*, 338–342.
(16) Greenblatt, M. *Chem. Rev.* **1988**, *88*, 31–53.

 Published on Web 04/20/2010

condense into layers via sharing of edges or vertices through bridging oxygen atoms.[17] While molybdenum and tungsten bronzes tend to be metallic, vanadium bronzes have narrower d-bands (due to the poorer overlap of 3d orbitals), and these compounds can therefore vary from semiconducting to metallic.[18−20]

Presented herein is a new vanadium bronze variant, $Cs_5FeV_5O_{13}Cl_6$, synthesized from the reaction of iron(III) oxides and V_2O_5 in the presence of a metal reducing agent, in molten CsCl/NaCl eutectic. This phase contains reduced vanadium oxide layers which are separated by $[FeCl_6]^{3-}$ anions and Cs^+ cations. Several characterization techniques indicate delocalization of electrons in the vanadate layer; this compound is therefore comprised of metallic vanadate layers separated by ionic Cs_3FeCl_6 slabs.

Experimental Procedure

Synthesis of $Cs_5FeV_5O_{13}Cl_6$. Iron(III) oxide (Strem Chemicals, 99.8%), vanadium(V) oxide (Strem Chemicals, 98+%), vanadium metal powder (Strem Chemicals, 99.5%), sodium chloride (Fisher Chemicals, 99.9%) and cesium chloride (Alfa-Aesar, 99.9%) were used as received without further purification. Vanadium(V) oxide (0.364 g, 2.00 mmol), iron(III) oxide (0.160 g, 1.00 mmol), and vanadium powder (0.0255 g, 0.500 mmol) were combined with a CsCl/NaCl eutectic mixture (13:7 molar ratio) equal to two times the mass of the reactants. The mixture was ground to a fine powder and placed in a fused silica tube. In order to dry the reactants and flux, the charged fused silica tube was placed in an oven and kept at 120 °C for two days before sealing under a vacuum of 1×10^{-2} Torr. The ampule was then heated to 650 °C in 3 h, cooled to 600 °C in 2 h, held at 600 °C for 48 h, cooled to 480 °C in 48 h, and finally cooled to room temperature in 12 h. Single crystals of $Cs_5FeV_5O_{13}Cl_6$ were isolated by washing the product quickly with deionized water using suction filtration.

Stoichiometric synthesis of this phase was also explored. In a glovebox, cesium chloride (2.525 g, 15 mmol), vanadium(V) oxide (1.310 g, 7.2 mmol), iron(III) oxide (0.160 g, 1.00 mmol), vanadium metal (0.031 g, 0.600 mmol), and iron(III) chloride (anhydrous, Fisher Chemicals, 98%; 0.162 g, 1.00 mmol) powders were ground together in a mortar and pestle and then sealed in a silica tube under vacuum. The mixture was heated to 750 °C in 6 h, held at this temperature for 24 h, and then cooled to room temperature in 24 h. Powder XRD data of the black powder product indicated it was predominantly $Cs_5FeV_5O_{13}Cl_6$, but additional diffraction peaks were also present from impurities which could not be identified (see Supporting Information).

Elemental Analysis. Elemental analysis was performed on the flux-grown crystals using a JEOL 5900 scanning electron microscope (SEM) with energy-dispersive spectroscopy (EDS) capabilities. The crystals were mounted on carbon tape and analyzed using a 30 kV accelerating voltage and an accumulation time of 10−20 s. Several crystals were analyzed to yield an average metallic element ratio of $Cs_5Fe_1V_5$, which is consistent with the X-ray data. The presence of both oxygen and chlorine was also confirmed; however, the molar ratios were not reliable.

Raman Spectroscopy. Raman spectra were obtained for $Cs_5FeV_5O_{13}Cl_6$ using a Jobin-Yvon Horiba LabRAM HR800 microRaman spectrograph with the 785 nm line of a TUIOptics DL 100 grating stabilized diode laser as the excitation source. Spectra were obtained using laser power of 15 mW (measured at the laser, around 1.5 mW at the sample). The laser beam was focused onto the sample through an objective (Leica 50x, 0.8 N. A.), which also collected the backscattered light.

Table 1. Crystallographic Data for $Cs_5FeV_5O_{13}Cl_6$

chemical formula	$Cs_5FeV_5O_{13}Cl_6$
fw (g/mol)	1395.72
space group	*P*4/*nmm*
a (Å)	10.943(3)
c (Å)	10.535(4)
V (Å)^3	1261.5(8)
d_{calcd} (g/cm^3)	3.67
Z	2
T (K)	298
radiation	Mo Kα
$2\theta_{max}$	56.83
reflections (total)	15 742
μ (mm^{-1})	6.69
R_1/wR_2 ($1 > 4\sigma(F°)$)	0.0340/0.0709
R_1/wR_2[a] (all data)	0.0418/0.0741
residual peak/hole (e$^-$/Å^3)	1.26/−1.99

[a] $R_1 = \sum(|F_o| - |F_c|)/\sum|F_o|$; $wR_2 = [\sum[w(F_o^2 - F_c^2)^2]/\sum(w|F_o|^2)^2]^{1/2}$.

Table 2. Atomic Coordinates and Isotropic Thermal Parameters (U_{eq})[a] for $Cs_5FeV_5O_{13}Cl_6$

atom	Wyckoff site	*x*	*y*	*z*	U_{eq} (Å^2)
Cs1	*2c*	0.5133(1)	0.9867(1)	0.2812(1)	0.0026(1)
Cs2	*8j*	1/4	1/4	0.3517(1)	0.0023(1)
V1	*8i*	0.5264(1)	1/4	0.0110(1)	0.0012(1)
V2	*2c*	3/4	3/4	0. 1497(2)	0.0014(1)
Fe1	*2b*	1/4	3/4	1/2	0.0018(1)
O1	*2c*	0. 6138(4)	0. 1138(4)	0	0.0023(1)
O2	*8i*	3/4	3/4	0. 3247(10)	0.0015(2)
O3	*8i*	0.4524(6)	1/4	0. 1432(6)	0.0030(1)
O4	*8 g*	0. 4234(5)	1/4	0. 8912(5)	0.0022(1)
Cl1	*8i*	0. 4705(2)	3/4	0. 5050(2)	0.0026(1)
Cl2	*4f*	1/4	3/4	0. 2740(3)	0.0032(1)

[a] U_{eq} is defined as one-third of the trace of the orthogonalized $\mathbf{U}_{ij}$ tensor.

Single Crystal and Powder XRD Measurements. Crystals for X-ray diffraction were selected from the SEM plate after elemental analysis. The crystals were mounted on glass fibers, and single crystal X-ray diffraction data were collected at room temperature using a Bruker AXS SMART CCD diffractometer equipped with a Mo radiation source. Processing of the data was accomplished with the use of the program SAINT; an absorption correction was applied to the data using the SADABS program.[21] Refinement of the structure was performed using the SHELXTL package.[22] During the final refinement cycles, the occupancy of all sites was allowed to vary to explore the possibility of partial or mixed occupancy, but none of the site occupancies varied significantly from unity. The crystallographic data are summarized in Tables 1 and 2; additional details regarding the crystallographic refinements can be found in the Supporting Information. Powder X-ray diffraction data was collected on the bulk sample to determine the yield and to identify the byproducts of the reactions. Samples were analyzed using a Rigaku Ultima III powder diffractometer. The MDI JADE 7.0 X-ray pattern data processing software was used to determine which phases were present and to calculate cell parameters.

Nuclear Magnetic Resonance. Magic angle spinning (MAS) NMR data were collected on a Varian Inova 500 widebore spectrometer. Crystals of $Cs_5FeV_5O_{13}Cl_6$ were first analyzed by EDS and then ground to a fine powder, which was then packed

(17) Hagrman, P. J.; Finn, R. C.; Zubieta, J. *Solid State Sci.* **2001**, *3*, 745–774.
(18) Wallis, R. H.; Sol, N.; Zylbersztejn, A. *Solid State Commun.* **1977**, *23*, 539–42.
(19) Kaplan, D.; Zylbersztejn, A. *J. Phys., Lett.* **1976**, *37*, 123–5.
(20) (a) Itoh, M.; Yamauchi, I.; Kozuka, T.; Suzuki, T.; Yamauchi, T.; Yamaura, J.-I.; Ueda, Y. *Phys. Rev. B: Condens. Matter Mater. Phys.* **2006**, *74*, 054434. (b) Ueda, Y. *Chem. Mater.* **1998**, *10*, 2653–2664.
(21) *SAINT*, version 6.02a; Bruker AXS, Inc.: Madison, WI, 2000.
(22) *NT/2000, S. 6.1*; Bruker AXS, Inc.: Madison, WI, 2000.

into a 4 mm zirconia rotor sealed with airtight screwcaps. The external reference for ^{51}V (I = 7/2, 99.76% abundant) was V_2O_5. Data were collected at room temperature with a spinning rate of 8 kHz, using a one-pulse sequence (pulse length 5 μs and relaxation delay 500 ms).

Magnetic Susceptibility. Magnetic measurements were carried out with a Quantum Design MPMS SQUID magnetometer at temperatures between 3 and 300 K. Crystals were first analyzed using EDS and single crystal XRD; several crystals (total mass 1.1 mg) were then were sealed in kapton tape and placed into the magnetometer. Temperature-dependent susceptibility data were collected at 100 G, and field dependence data were collected at 3 K.

Results and Discussion

Layered vanadate compounds are of great interest due to their potential applications as catalysts, battery electrodes, and magnetic materials.[23−26] Vanadium can adopt several oxidation states and different coordination modes; as a result, vanadates exhibit great structural versatility.[17] Metal halide flux synthesis appears to be a promising technique for growth of these phases. However, halide salts do not always behave as inert solvents. An intriguing example of this is the series of salt-inclusion vanadate phases with the general formula $[(AX)_2Mn(VO_3)_2]$ (A/X = Cs/Cl, Cs/Br, Rb/Cl) and $[(CsCl)Mn_2V_2O_7]$ synthesized from the reaction of metal oxides in AX and CsCl/NaCl eutectic, respectively.[6] Vanadium has a +5 oxidation state in all these compounds. Lower-valent vanadium is found in hybrid layered vanadates, such as M(bipyridine)V_4O_{10} (M = Cu, Ag), synthesized using hydrothermal methods with a nitrogenous base (bipyridine) acting as the reducing agent.[27] These compounds have partially reduced vanadate layers linked together by organic bridges, and they exhibit interesting magnetic phenomena, such as spin ladder formation.[27,28] Our compound falls between these two classes of layered vanadates. In our exploration of reactions of metal oxides and metal powder in molten salts, we have isolated a new reduced vanadate salt-inclusion compound grown in the CsCl/NaCl flux mixture.

The 13:7 molar ratio of CsCl and NaCl forms a eutectic which melts at 495 °C. The reaction of V_2O_5, Fe_2O_3, and vanadium metal in the CsCl/NaCl melt results in the formation of the title phase, $Cs_5FeV_5O_{13}Cl_6$; this forms in approximately 60% yield based on vanadium, with the remaining vanadium incorporated into byproducts, such as the ternary phases $CsVCl_3$ and $Cs_2V_4O_{11}$.[29,30] Crystals of $Cs_5FeV_5O_{13}Cl_6$ can also be grown from the reaction of V_2O_5, $BaFe_{12}O_{19}$ and iron metal in CsCl/NaCl flux, which confirms that the metal (V or Fe) acts as a reducing agent and is required for the formation of the product. The metal oxides (V_2O_5, Fe_2O_3, or $BaFe_{12}O_{19}$) dissolve in the CsCl/NaCl melt; the metal powder (Fe or V) facilitates the reduction of the vanadium, which subsequently leads to the formation of the $Cs_5FeV_5O_{13}Cl_6$ phase. Similar flux reactions of vanadium metal and V_2O_5 in the absence of a source of iron lead to formation of powdered vanadium suboxides, such as V_2O_3 and $VO_{0.53}$. $Cs_5FeV_5O_{13}Cl_6$ grows as dark plate-like crystals with metallic shine which do not decompose upon exposure to air. This phase is somewhat sensitive to water. Attempts to separate the product from the solidified salt flux by extended soaking in water leads to degradation after several hours, but the product is stable enough to be isolated using a quicker water rinse with suction filtration. This phase can be made from stoichiometric synthesis, but the powder XRD data indicates the presence of impurity phases (see Supporting Information), so all characterization was carried out on flux-grown crystals.

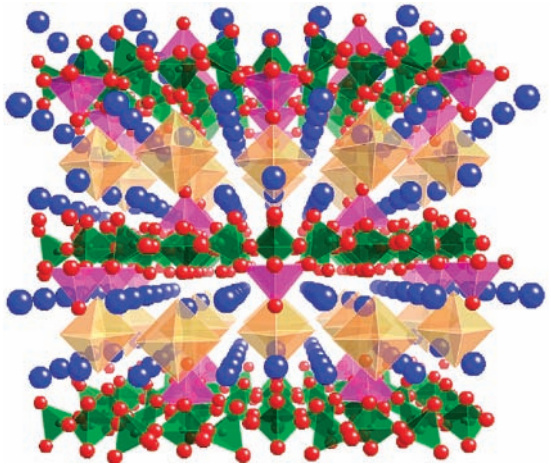

Figure 1. The structure of $Cs_5FeV_5O_{13}Cl_6$, viewed down the a-axis, showing the vanadate layers (red and green polyhedra) separated by $[FeCl_6]^{3-}$ octahedra (tan) and cesium cations (blue).

Structure of $Cs_5FeV_5O_{13}Cl_6$. The crystal structure of $Cs_5FeV_5O_{13}Cl_6$ is shown in Figure 1. This compound crystallizes in the tetragonal space group $P4/nmm$ and exhibits a novel two-dimensional (2D) structure comprised of puckered vanadate layers, $[V_5O_{13}]^{2-}$, stacked in an eclipsed fashion along the c-axis and separated by Cs^+ cations and $[FeCl_6]^{3-}$ octahedra. The octahedra contain four longer Fe−Cl bonds of 2.4137(2) Å and two shorter Fe−Cl bonds of 2.3806(3) Å. These bond distances are in the range expected for a Fe(III)−Cl bond, indicating a +3 oxidation state for the iron cation.[31,32] Each face of the octahedron is capped by a cesium cation; these cations are also coordinated by oxygen atoms capping the vanadate layer.

The vanadate layer, shown in Figure 2, consists of corner-sharing tetrahedral VO_4 and square pyramidal VO_5 units (shown as green and red polyhedra), which are connected via bridging oxygen atoms. There are two unique vanadium sites in the crystal structure of $Cs_5FeV_5O_{13}Cl_6$. V1 is in the +5 oxidation state and is tetrahedrally coordinated to four oxygen atoms with two shorter V−O bonds at a distance of ~1.6115−1.6920 Å and two longer V−O bonds of 1.7746(1) Å (Table 3). V2 is

(23) Livage, J.; Bouhedja, L.; Castro-Garcia, S.; Julien, C., *Mater. Res. Soc. Symp. Proc.* **1999**, 548, (Solid State Ionics V), 161-172.
(24) Xu, H. J.; Wang, Z. L.; Yao, K. L. *Phys. B (Amsterdam, Neth.)* **2009**, *404*, 1729–1732.
(25) Maggard, P. A. Abstracts. Proceedings of 62nd Southwest Regional Meeting of the American Chemical Society, Houston, TX, October 19−22, 2006; SRM-079.
(26) Xiao, D.; Xu, Y.; Hou, Y.; Wang, E.; Wang, S.; Li, Y.; Xu, L.; Hu, C. *Eur. J. Inorg. Chem.* **2004**, *7*, 1385–1388.
(27) Yan, B.; Maggard, P. A. *Inorg. Chem.* **2007**, *46*, 6640–6646.
(28) Yan, B.; Olmstead, M. M.; Maggard, P. A. *J. Am. Chem. Soc.* **2007**, *129*, 12646–12647.
(29) Hauser, A.; Guedel, H. U. *Chem. Phys. Lett.* **1981**, *82*, 72–75.
(30) Oka, Y.; Saito, F.; Yao, T.; Yamamoto, N. *J. Solid State Chem.* **1997**, *134*, 52–58.
(31) Segal, B. M.; Hoveyda, H. R.; Holm, R. H. *Inorg. Chem.* **1998**, *37*, 3440–3443.
(32) Jutzi, P.; Neumann, B.; Schebaum, L. O.; Stammler, A.; Stammler, H.-G. *Organometallics* **2000**, *19*, 1445–1447.

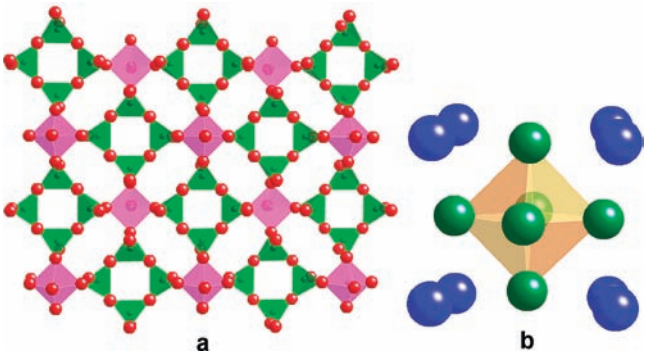

Figure 2. (a) The vanadate layer of $Cs_5FeV_5O_{13}Cl_6$ viewed down the *c*-axis. Pink polyhedra = $V^{(IV)}O_5$, green polyhedra = $V^{(V)}O_4$, and red = oxygen. (b) $[FeCl_6]^{3-}$ octahedron.

Table 3. Selected Bond Lengths (Å) for $Cs_5FeV_5O_{13}Cl_6$

bond	length (Å)
V(1)−O(2) × 1	1.6115(6)
V(1)−O(3) × 1	1.6920(5)
V(1)−O(4) × 2	1.7746(1)
V(2)−O(1) × 1	1.8440(1)
V(2)−O(3) × 4	1.9458(5)
Fe−Cl(1) × 2	2.3806(3)
Fe−Cl(2) × 4	2.4137(2)

in the +4 oxidation state and is coordinated to five oxygen atoms in a square pyramidal configuration with one short apical V−O bond at a distance of 1.8440(1) Å and four longer basal V−O bonds at a distance of 1.9458(5) Å (Table 3). Other layered vanadate structures show similar V−O distances.[6,17] The assigned oxidation states agree with the observed bond lengths (the V^{5+} site has shorter V−O bonds than the V^{4+} site); they also result in a suitable charge balance for the compound $(Cs_5(Fe^{3+})(V^{4+})(V^{5+})_4O_{13}Cl_6)$. Calculated bond valence sums indicate oxidation states of +5.18 and +3.62 for V1 and V2, respectively.[33,34] The Raman spectrum collected on a single crystal of $Cs_5FeV_5O_{13}Cl_6$ contains an intense peak at 890.3 cm^{-1}, which corresponds to the terminal (V=O) stretching mode of the tetrahedral $V^{5+}O_4$ units; this bond length is 1.6115(6)Å, which should produce a Raman mode of around 900 cm^{-1}.[35] Weaker Raman peaks appear in the range of 615−770 cm^{-1}, likely corresponding to V−O stretching and bending modes of bridging oxygen atoms (see Supporting Information).[35]

In the vanadate sheets, the reduced VO_5 square pyramids are structurally isolated from each other and connected to VO_4 tetrahedra through bridging oxygen atoms. The disparity in the bond lengths around the two vanadium sites and the large difference in resulting bond valence sums point to localization of the d-electrons on the V^{4+} sites. However, the metallic shine of the crystals suggests the delocalization of the electrons across the entire vanadate layer. Since the crystals were too small to allow for resistivity measurements, ^{51}V NMR and magnetic susceptibility data were collected to gain further information on the electronic properties of this system.

NMR Data. MAS NMR measurements were carried out to explore the possible presence of delocalized electrons and their effect on the chemical shift of the vanadium sites in $Cs_5FeV_5O_{13}Cl_6$. There are two nonequivalent vanadium sites in the crystal structure: tetrahedral V^{5+} and square pyramidal V^{4+}. These two vanadium sites should lead to two peaks in the ^{51}V NMR spectrum. However, only one peak is observed. This is possibly due to peak broadening from the large quadrapole moment of the vanadium nucleus; if the chemical shifts of the two peaks are similar, then they may overlap and become difficult to distinguish. Another possibility is that one of the peaks might be extensively broadened due to fast relaxation caused by the delocalized electron in the vanadate layer and by the presence of a nearby Fe^{3+} paramagnetic ion and might not be evident in the spectrum.

The ^{51}V isotropic chemical shift observed for $Cs_5FeV_5O_{13}Cl_6$ appears at 5170 ppm (referenced to V_2O_5 at 0 ppm; see Supporting Information). The magnitude of the shift is much larger than the negative or small positive values seen for insulating or semiconducting vanadium phases, such as $(C_{10}H_{10}N_2)[(VO_2)_4(PO_4)_2]$ (∼ 590 ppm)[36] and $V_2S_4(S_2COEt)_4$ (70 ppm),[37] and is very close to the chemical shift of vanadium metal (5200 ppm),[37] suggesting a metallic nature for this compound. The interaction of conduction electrons with an applied magnetic field produces an extra effective field on the nuclear magnetic moment, resulting in a large paramagnetic shift—the Knight shift.[38] Previously observed isotropic chemical shifts for vanadium bronzes fall in the range of −435 ppm for $Ag_{0.35}V_2O_5$ to 2120 ppm for $Ca_{0.3}V_2O_5$.[37] The isotropic chemical shift of 5170 ppm is at a much lower field than expected. In combination with the magnetic susceptibility data, this indicates that the electrons on the V^{4+} ions are delocalized throughout the vanadate layers. In addition to the effects of conduction electrons, the presence of localized electrons on nearby Fe^{3+} ions may also contribute to the shift.

Magnetic Susceptibility Measurements. There are two potentially paramagnetic ions in $Cs_5FeV_5O_{13}Cl_6$: Fe^{3+} and V^{4+}. However, overlap of the d-orbitals of vanadium may result in band formation, allowing the unpaired electron on the V^{4+} ions to be delocalized. If this is the case (as is indicated by the NMR data), then only the electrons on the iron ions will behave as localized paramagnets; the delocalized electrons in the vanadate layers will only contribute a small temperature-independent Pauli paramagnetism to the susceptibility. Temperature-dependence data are shown in Figure 3. The material shows Curie−Weiss behavior at high temperatures; fitting the inverse susceptibility data to the Curie−Weiss equation yields a Curie constant $C = 3.55(1)$ emu·mol^{-1} K and a Weiss constant $\theta = -5.9(2)$ K. From the Curie constant, the calculated effective magnetic moment per formula unit is equal to 5.35(1) μ_B, which is in agreement with the expected spin-only value for high-spin Fe^{3+}

(33) Brese, N. E.; O'Keeffe, M. *Acta Crystallogr., Sect. B: Struct. Sci.* **1991**, *B47*, 192–7.
(34) Brown, I. D.; Altermatt, D. *Acta Crystallogr., Sect. B: Struct. Sci.* **1985**, *B41*, 244–7.
(35) Hardcastle, F. D.; Wachs, I. E. *J. Phys. Chem.* **1991**, *95*, 5031–41.
(36) Shi, F.-N.; Paz, F. A. A.; Rocha, J.; Klinowski, J.; Trindade, T. *Eur. J. Inorg. Chem.* **2004**, *15*, 3031–3037.
(37) Lapina, O. B.; Khabibulin, D. F.; Shubin, A. A.; Terskikh, V. V. *Prog. Nucl. Magn. Reson. Spectrosc.* **2008**, *53*, 128–191.
(38) Carter, G. C.; Bennett, L. H.; Kahan, D. J. Metallic Shifts in NMR. In *Progress in Materials Science*; Pergamon Press: New York, NY, 1977; *Vol. 20*.

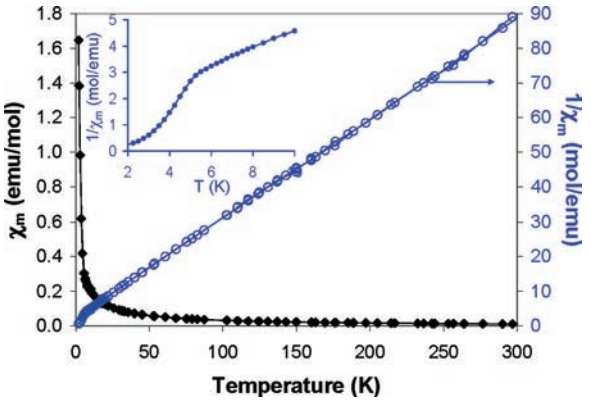

Figure 3. Temperature dependence of the magnetic susceptibility (right axis, black symbols) and inverse susceptibility (left axis, blue symbols) of $Cs_5FeV_5O_{13}Cl_6$, showing Curie−Weiss behavior at high temperature. Inset: Low-temperature inverse susceptibility, highlighting the ferrimagnetic transition at 5 K.

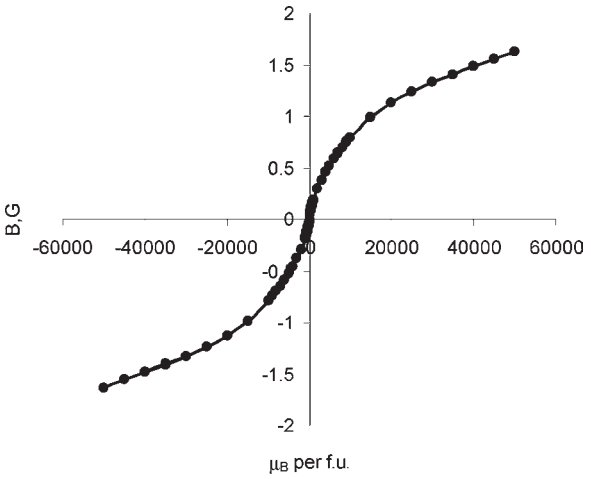

Figure 4. Magnetization versus field data for $Cs_5FeV_5O_{13}Cl_6$, collected at 2 K.

(theoretical value 5.9 μ_B). The V^{4+} ions are clearly not contributing significantly to the magnetic moment; this confirms that their electrons are delocalized at high temperatures.

$Cs_5FeV_5O_{13}Cl_6$ appears to order ferromagnetically at low temperatures, indicated by a sharp increase in the susceptibility at 5 K. The magnitude of the Weiss constant is in agreement with the observed transition temperature. However, the negative sign may indicate antiferromagnetic coupling between inequivalent magnetic sublattices, leading to overall ferrimagnetic behavior. Localization of the electrons in the vanadate layer at low temperature may provide a second magnetic sublattice which couples antiferromagnetically with the Fe^{3+} moments in the ionic layer. Magnetization data below the transition were collected to gain further insight on the ordering (Figure 4). This data shows an S-shape dependence on field, but no saturation is reached at the highest applied magnetic field (6 T). No hysteresis or metamagnetic transitions are observed. The maximum value of the magnetization is small, supporting the idea of ferrimagnetic ordering. If the magnetic moments of Fe^{3+} and V^{4+} are partially canceled by antiferromagnetic coupling between these ions, then this will result in a small net moment per formula unit.

Further low-temperature structural and magnetic measurements are necessary to confirm the origin and the nature of the observed magnetic ordering transition in $Cs_5FeV_5O_{13}Cl_6$. The iron(III) centers in the ionic layer are far apart (7.7 Å Fe−Fe distance), and direct coupling is unlikely (as is superexchange coupling, given the lack of directly bridging ligands). However, it is notable that antiferromagnetic coupling is observed at 6.6 K in $Cs_2[FeCl_5(H_2O)]$, a compound featuring iron-centered octahedra linked only by hydrogen bonding (with a 7.1 Å Fe−Fe distance).[39] The nature of the magnetic coupling in $Cs_5FeV_5O_{13}Cl_6$ is likely complex, with RKKY coupling via the conduction electrons in the vanadate layers (or coupling with the V^{4+} moments if localization of the conduction electrons occurs at low temperature) possibly contributing to the ordering of the iron sublattice. Full understanding may require advanced techniques, such as neutron diffraction.

Conclusions

Molten salts are a promising media for the growth of single crystals of subvalent metal oxide compounds. A variety of metals (Fe, V, Co, Mo) appear to be effective reducing agents for early transition-metal oxides in salt fluxes. The mechanism of such reactions is not known yet; however, one can propose that first metal oxides dissolve in the molten salt; this liquid phase contacts the metal allowing for reduction, and upon cooling, the reduced oxide framework forms around cations and other ionic species in the salt flux.[6,40] Variations in molten salt solvent, reaction temperature, and stoichiometry may determine the extent of inclusion of salt species in the product structure. We are currently expanding this chemistry to molybdate systems.

Acknowledgment. We thank Dr. Randall Achey for his assistance with MAS NMR spectroscopy and Dr. Bert van der Burgt for his assistance with the Raman spectroscopy. We thank Dr. Michael Shatruk for helpful discussions regarding the magnetism aspects of this work. This research was supported by the Florida State University (FSU) Department of Chemistry and Biochemistry and by the National Science Foundation (grant number DMR-05-47791). This work made use of the SEM facilities of MARTECH at FSU.

Supporting Information Available: Raman spectrum, ^{51}V MAS NMR data, and powder XRD pattern for $Cs_5FeV_5O_{13}Cl_6$. Crystallographic information in CIF format. This material is available free of charge via the Internet at http://pubs.acs.org.

(39) (a) O'Connor, C. J.; Deaver, B. S.; Sinn, E. *J. Chem. Phys.* **1979**, *70*, 5161–5167. (b) Palacio, F.; Paduan-Filho, A.; Carlin, R. L. *Phys. Rev. B: Condens. Matter Mater. Phys.* **1980**, *21*, 296–298.

(40) La Violette, R. A.; Budzien, J. L.; Stillinger, F. H. *J. Chem. Phys.* **2000**, *112*, 8072–8078.